Paweł OSTAPKOWICZ[*]

SENSITIVITY ASSESSMENT OF A GRADIENT-BASED LEAK LOCALIZATION PROCEDURE FOR PRESSURE SENSOR FAULTS USING A LABORATORY MODEL OF A TRANSMISSION PIPELINE

Summary. This research addresses the topic of leakage localization in liquid transmission pipelines. Particularly, it deals with the standard gradient-based procedure used for performing such a task. The procedure relies on pressure gradient calculations based on pressure data collected from measurement points distributed along the pipeline. This study aimed to verify this procedure regarding its sensitivity to typical systematic errors related to pressure transducers. The primary measure evaluated was the accuracy of the calculated coordinate of a leak spot. The uncertainty of the leak localization result was also estimated following the Guide to the Expression of Uncertainty in Measurement convention. A laboratory model of the pipeline was used to practically implement and test the procedure. During experiments, low-intensity leakages with a level of 0.25–2.00% were simulated. Regarding typical systematic errors, the bias (zero moving) type and the proportional ratio type were considered, which were numerically simulated in the measurement data. The findings reveal how sensitive the examined procedure is in relation to these errors, considering their different levels and scenarios related to used pressure transducers.

1. INTRODUCTION

Transport is a pillar of the functioning and development of many industries, including power industry and trade. Regardless of the kind of goods transported, the infrastructure and means of transport are important. This also applies to a significant task, which is the transportation of liquids over long distances. Such a task is usually a great challenge. In practice, it can be implemented through road, rail, maritime, and pipeline transport. Under some circumstances involving large-scale transferring, transmission pipelines appear to be the best and most effective solution. Such pipelines have high scores on key factors, such as capacity, expenditures, reliability, safety, and ecological impact.

Owing to their operation structure and durability, pipelines can also withstand different and tough environmental conditions and interactions with other transport modes. This ensures delivery continuity and long-term use. Pipelines have a high capacity, which favorably balances the high initial costs of construction and launching new pipelines. Finally, pipelines also have low unit costs (per ton per kilometer).

As a result, transmission pipelines are a common mode of transport for many liquid substances, including those of strategic importance, such as petroleum and its products as well as water, between various phases or stages of extraction, production, processing, storage, and distribution.

Transmission pipelines operate under high pressure and pose a risk of leakage of the pumped medium outside the pipe. Leakage can result in severe environmental threats and public impacts, as well as substantial economic losses. Such a risk can be considerably mitigated by applying the right solutions at the design and construction phase of the pipeline. For instance, they can aim to increase the corrosion resistance of the pipeline or to balance or compensate for the stresses in the pipeline material caused by

---

[*]Bialystok University of Technology, Faculty of Mechanical Engineering; Wiejska 45C, 15-351 Bialystok, Poland; e-mail: p.ostapkowicz@pb.edu.pl; orcid.org/0000-0003-0430-4696

temperature changes. Moreover, important measures are taken during the operation phase of the pipeline, which mainly aim to preserve the technical condition of the pipeline [11]. Such actions involve, for example, the modification of the dynamic characteristics of the pipe-pump system for vibration damping [14]. Other important issues include the use of the non-contact method for estimating the stress-strain state of pipelines located below ground [4] and the assessment and foresight of the rate of erosion wear of pipe walls caused by the flow of the pumped medium [1]. Depending on the surroundings of the pipeline, it may also be helpful to evaluate its reliability for specific types of external interactions (e.g., rockfall impact) [13], or other interactions caused by chemical and thermal factors as well as the pressure inside the pipe [8]. It may also be helpful to analyze the efficiency of transport, taking into account issues in the field of optimization and mitigating risks through their appropriate management [2].

However, the risk of leakage cannot be completely avoided for liquid transmission pipelines. This may be due in part to frequent occurrences of theft of the pumped medium from the pipeline or damage of the pipe, which can be deliberate or accidental.

Hence, in order to reduce the effects of leak occurrence, liquid transmission pipelines are equipped with leak detection systems (LDSs). LDSs can use external (direct, or hardware-based) diagnostic methods to identify leaks from the outside of the pipe. This can be done with special devices, such as microphones, hydrocarbon detectors, and thermal cameras [6]. However, another type of diagnostic method is also crucial. These are analytical (internal, indirect, or software-based) methods, which are based on measurements of flow parameters in a pipeline, such as mass/volume flow, pressure, and temperature. The development of the above analytical methods, in addition to the detection and location of leakage, makes it possible to estimate its intensity. In practice, each of these tasks requires a distinct analytical method.

Pipeline operators expect an LDS to be able to locate the leak spot precisely. Operators also want this to happen as fast as possible from the moment when a detection algorithm signals a leak. These expectations apply not only to large leaks but also to those of less than 1% nominal flow intensity, which are hard to diagnose. Suitable leak localization methods are needed to meet these expectations. These methods are reviewed in [6, 10].

The use of any analytical method involves potential complex combinations of uncertainties (errors). They can affect instrumentation, the model of a pipeline, and data processing. Meanwhile, other causes cannot be ignored, such as disturbances and changes in the flow, as well as noises, distortions, and even gaps in measurement data, as they can hinder a system's ability to produce a correct final diagnosis.

The task of leak location can be particularly challenging because the pipeline operator relies on the calculated leak location coordinate to make decisions. These include locking certain valves to cut off the damaged pipeline section and sending repair teams to find and repair the pipe damage. Therefore, when the leak location result is uncertain, the operator needs some indication of its uncertainty.

The literature contains examples of research on the effect of many input variables on the uncertainty of diagnostic functions. This applies to detection algorithms [5] and the frequent use of leak location procedures that employ the negative pressure wave formation and propagation phenomenon in a pipeline caused by a leak [3, 7].

The author also participated in research on another widespread standard gradient leak localization procedure [9, 12]. This procedure is used in both simple and advanced analytical methods. The research considered the uncertainty of the calculated leak location coordinate that depends on the metrological characteristics of measuring devices and measurement conditions. The investigation assumed that the measurement data were free of field instrumentation defects as well as data transmission gaps or discontinuities.

However, the pressure measurement system installed on the transmission pipeline may not always work correctly. The system collects pressure measurement data from points at the inlet and outlet as well as from some additional points along the pipeline. These points are usually far from the system headquarters or command center. It should also be noted that checking the accuracy of each measurement channel of the system involves applying very complex testing procedures that require specialist tools and many competent personnel. Because these tests are conducted at specific intervals, during the time between them, the measurement system may operate with errors. One of the significant

components of the measurement channel that could be affected by damage is analog pressure transducers.

This study evaluates the sensitivity of the above-mentioned standard leakage localization procedure to several typical systematic errors in analog pressure transducers. These errors are assumed to have the ability to indicate a defect in the measuring device.

2. STANDARD GRADIENT-BASED LEAK LOCALIZATION PROCEDURE

Let us consider a simple, horizontal pipeline with a length z defined in terms of the coordinate z. This pipeline is made of pipes with the same internal diameter, $d(z) = const$.

Suppose the pipeline is leakproof, that the flow of the incompressible fluid being pumped through it is single-phase and isothermal, and that it proceeds under stationary conditions with insignificant mass accumulation values within the pipe volume. Then, the pressure distribution along the pipeline can be described by a straight line, as shown by the green line in Fig. 1.

However, if damage occurs at a location with the coordinate z_u resulting in the release of fluid with an intensity q_u, this will cause dynamic (transient) changes in pressure and flow. After a certain time, these fluctuations stabilize and evolve into a new steady state whose pressure distribution is expressed by two straight lines that intersect exactly at the leak point, as shown by the red line in Fig. 1.
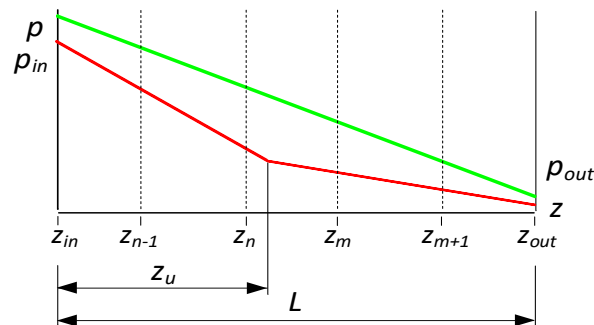
Fig. 1. Distribution of pressure in no-leak conditions (green line) and after leak occurrence (red line)

The researched standard gradient-based leak localization procedure requires the abscissa of the intersection point between two straight lines to be determined. This calculation is completed using the following formula:

$$z_u = \frac{p_{out} - p_{in} - G_{out} \cdot L}{G_{in} - G_{out}}$$

(1)

where: L – length of the examined pipeline' section; p_{in}, p_{out} – pressure after the leak occurrence for the initial and final cross-section of the examined pipeline' section; G_{in}, G_{out} – pressure gradients after the leak occurrence in subsections of the pipeline before and behind the leak spot.

In practical implementation, this leak localization procedure (1) relies on the data gathered from pressure sensors. These sensors should be deliberately arranged at both the inlet and outlet of the pipeline, as well as at several points along the pipeline. Specifically, at least four pressure sensors are required: two in front of the suspected leak point and two behind it. Whenever feasible, it is desirable to select sensors that are spaced as far as possible from each other.

3. ACCURACY AND UNCERTAINTY OF THE LEAK LOCALIZATION PROCEDURE

The accuracy of the leak location procedure (1) can be computed by the error representing the difference between the estimated and real location of the leak using the following formula:

$$ER_u = \hat{z}_u - z_u \tag{2}$$

The uncertainty of the estimated coordinate of the leak point according to Expression (1) is determined by the combined standard uncertainty. This evaluation follows the guidelines outlined in the Guide to the Expression of Uncertainty in Measurement (GUM) [15] and the ISO 5168 standard [16].

Notably, the input quantities required for leak point calculations include measured pressures p_{in}, p_n, p_m, p_{out}. These pressures are assumed to be uncorrelated. The standard uncertainties associated with these pressure variables are estimated based on repeated pressure measurements. These uncertainties are composed of two components: Type A standard uncertainty (resulting from statistical variations) and Type B standard uncertainty (arising from systematic effects), as described by Relationship (3).

$$u(p) = \sqrt{[u_A(p)]^2 + [u_B(p)]^2} \tag{3}$$

Initially, the standard uncertainties calculated for the individual measured pressures p_{in}, p_n, and p_m, p_{out}, are employed to assess the uncertainties associated with gradients G_{in} and G_{out}, respectively.

Finally, the overall uncertainty of the standard leak location procedure (1) can be estimated using the following formula:

$$u(z_u) = \sqrt{[u(p_{in})c(p_{in})]^2 + [u(p_{out})c(p_{out})] + [u(G_{in})c(G_{in})]^2 + [u(G_{out})c(G_{out})]^2 + [u(L)c(L)]^2} \tag{4}$$

where: $u(p_{in})$, $u(p_{out})$ – uncertainties of the estimated pressures p_{in} and p_{out}; $u(G_{in})$, $u(G_{out})$ – uncertainties of the calculated pressure gradients G_{in} and G_{out}; $u(L)$ – uncertainty of the distance' measure between the extremes of the examined pipe; $c(...)$ – individual sensitivity coefficients calculated as partial derivatives.

4. ERRORS OF ANALOG PRESSURE SENSORS

The assessment of the sensitivity of the investigated procedure pertains to input quantities linked to pressure measurements within a pipeline. Specifically, this relates to the incorrect functioning of analog pressure sensors caused by widespread systematic errors of a static nature.

4.1. Common errors of analog pressure sensors

The defects that concern analog pressure sensors are primarily the ones of potential malfunctions in the measuring systems used for liquid transmission pipelines. When employing analog pressure sensors as measurement devices, the errors observed in their outputs can be categorized as either dynamic or static. For instance, the measurement drift is numbered among dynamic errors.

An ideal static characteristic for an analog pressure sensors is indicated by the dotted lines in Fig. 2. However, in practice, the sensor exhibits a specific level of accuracy resulting from systematic errors. A useful parameter for assessing systematic error is the limiting uncertainty Δp. Typically, this uncertainty band Δp is estimated based on the maximum absolute measurement error, as detailed in the manufacturer's manuals. Linking this value to the measurement range makes it possible to determine the instrument's accuracy class.

We assume that a properly functioning pressure sensor with a defined accuracy level Δp may reveal various systematic errors. Overall, these errors should not significantly deviate from the accepted margins $(p - \Delta p, p + \Delta p)$, where the pressure p corresponds to the previously mentioned ideal static characteristics.

In this study, we focus on two typical systematic errors of the static type: the zero-point (bias) error (illustrated by the solid line in Fig. 2a) and the gain error (illustrated by the solid line in Fig. 2b). These

errors involve the displacement and divergence (deviation) of the measuring properties of the sensor from its theoretically "ideal" distribution (dotted line).
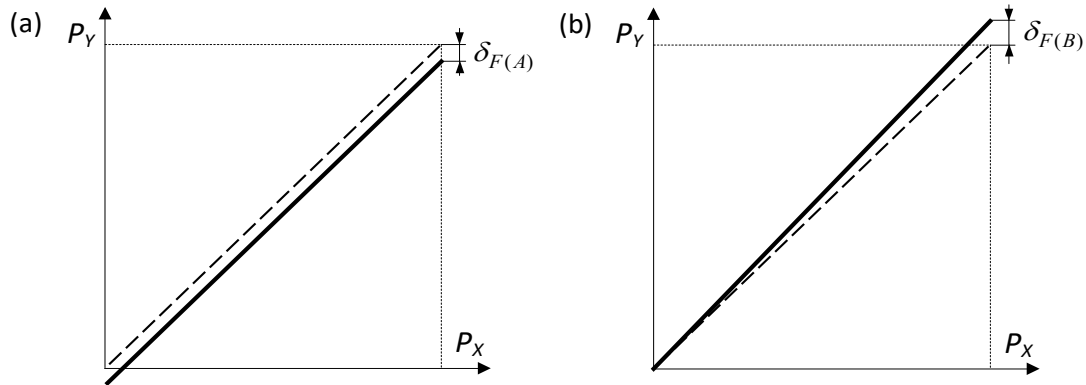
Fig. 2. Static characteristics of the pressure sensor (with the effect of the digitalization process omitted) as a relation of the output measuring variable "P_Y" with respect to the real measuring variable "P_X": an ideal one (dotted line) and other ones (solid lines) corresponding to the errors of bias (zero moving) type (a) and gain type (b)

4.2. The considered structure of measuring channels

Transmission pipelines, due to the distribution of individual pressure measurement points, need to use dispersed measurement systems. These systems are essential for gathering measurement data across distances that, towards the system headquarters, can range from a few up to several dozen kilometers. In practical terms, the above conditions result in a complex hardware configuration for measuring channels within the system. In addition to measuring sensors, this configuration may encompass other components such as A/D signal converters and modules for wired or wireless transmission.

In this study, we focus on a simplified measuring channel structure that combines an analog pressure transducer with an A/D signal converter (see Fig. 3).
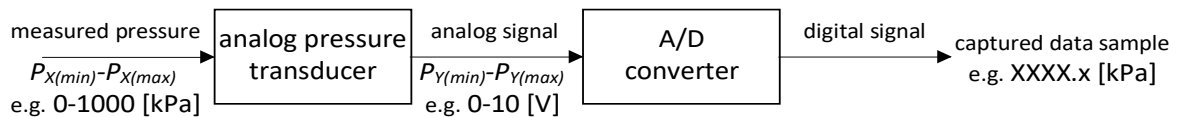
Fig. 3. Structure of measuring channels

Such a system enables the acquisition of digital data samples. This is in line with the broad concept of analytical methods whose diagnosis results are derived through computer processing of these data samples. The collected data samples, as a result of the measurement, are characterized by a specific resolution. Their accuracy can be expressed as $\Delta p_\Sigma = \Delta p + \Delta p_{A/D}$, where Δp represents the limiting uncertainty of analog pressure transducer and $\Delta p_{A/D}$ corresponds to the limiting uncertainty of A/D converter.

5. EXPERIMENTAL VERIFICATION OF THE LEAK LOCALIZATION PROCEDURE

In order to verify the impact of pressure sensor errors on the efficiency of the leak localization procedure under discussion, we applied measurement data acquired from tests conducted on a laboratory model of a pipeline.

5.1. The laboratory pipeline

The laboratory pipeline setup (Fig. 4) is located at the Faculty of Mechanical Engineering, Bialystok University of Technology in Poland. This physical model simulates a water pipeline and includes a main pipe section, a variable flow pump, and two semi-open tanks (located at the inlet and outlet), each with a capacity of 300 dm^3. The entire pipe duct spans approximately 400 m, including a 380-m-long main pipe section (between coordinates $z = 0$ and $z = 380$). The main pipe is constructed from polyethylene tubes (HDPE) with an internal diameter of 34 mm and an external diameter of 40 mm.

Fig. 4. Laboratory model of the pipeline

5.2. Pressure measurement system

To obtain pressure measurements in the laboratory pipeline, we employed analog pressure transducers placed at specific coordinates: 1 m, 61 m, 141 m, 201 m, 281 m, and 341 m. These pressure transducers were connected to a PC via a 16-bit A/D converter. Each measuring channel within the pressure measurement system corresponded to the hardware configuration depicted in Fig. 3. It should be noted that all the pressure transducers were characterized by identical input and output ranges, with extreme values consistent with those shown in Fig. 3. Furthermore, their accuracy was defined by upper and lower limits of maximum absolute errors, both of which were equal to $\Delta p = 1.0$ kPa. The A/D converter's associated errors were similarly assumed to be $\Delta p_{A/D} = 0.2$ kPa based on information provided in the manufacturer's manuals.

5.3. Conditions of experiments with simulated leakages

During experimental tests conducted on this pipeline, we focused on single low-intensity leakages occurring at three specific points: 75 m, 155 m, and 235 m along the pipeline. These locations correspond to the inlet, middle, and outlet sections of the pipeline. To simulate these leaks, we employed solenoid valves equipped with interchangeable diameter orifices.

The pipeline was operating in a steady state before a leak was initiated by suddenly opening the designated solenoid valve through a step change in the control signal. The simulated leak sizes ranged from approximately 0.25% to 2.00% of the nominal flow rate value. The temperature of the pumped water varied between 15 and 25 °C.

Throughout the tests, we sampled data related to all measured pressures at a frequency of $f_P = 100$ Hz, collecting them with a resolution of 0.1 kPa.

5.4. Faults (errors) introduced into the measurement system

The correctness of the measuring system concerning the recorded pressure values within the pipeline was preliminarily tested using a specialized setup (Fig. 6). This system comprised a straight pipe segment connected to the pump system, with shut-off valves positioned at both ends. The test pipe was equipped with mounting seats for pressure sensors under examination. By adjusting specific pressure values, assumed to be equivalent to the entire pipe volume, we evaluated the measuring channels connected with individual pressure sensors.

Fig. 5. System used for testing individual measuring channels with the visible joints for installation of pressure sensors

Regarding the two potential errors related to pressure sensors, their actual occurrence could be triggered by interventions in electronic systems or the use of an external system simulating changes in the output signal. Nevertheless, it is fundamental to assess system performance both with and without simulated damage. Furthermore, given the low intensity of leaks, flow disturbances are likely to significantly impact the estimated values corresponding to measured pressures. To ensure examination credibility, each experiment related to a specific leak location and the size of the simulated leak should be conducted keeping the repeatability of pipeline operating conditions. In practice, this can necessitate multiple repeat attempts.

Consequently, it was determined that two specific types of systematic errors would be simulated numerically rather than through hardware modifications. These errors were intentionally introduced into pressure data samples. By doing this, we expected to replicate a warning state in the operation of a pressure sensor. Such a created state is considered in relation to the originally correct operation of a sensor that was characterized by the specified accuracy margin Δp. It is worth recalling that this method of simulating errors (faults) is merely a rough approximation of their real impact.

The first type of error, known as bias (zero moving) error, was individually simulated for each of the individual pressure sensors p_{in}, p_n, p_m, p_{out}. These sensors are taken into account when calculating the coordinates of leak points according to Formula (1). The error levels, as depicted in Fig. 2a, were $\delta_{F(A)} = -0.2$ kPa and $\delta_{F(A)} = -0.5$ kPa. The upper value corresponds to half of the limiting uncertainty Δp associated with the pressure transducers used, while the lower value is twice as large as the resolution of the collected data samples.

The second type of error, referred to as gain error, was simultaneously simulated for all pressure sensors (p_{in}, p_n, p_m, p_{out}). These errors are tied to the nominal characteristics of the pressure sensor. Specifically, their assumed measures, as depicted in Fig. 2b, were $\delta_{F(B)} = 0.2$ kPa, $\delta_{F(B)} = 0.5$ kPa, $\delta_{F(B)} = 1.0$ kPa, $\delta_{F(B)} = 2.0$ kPa, $\delta_{F(B)} = 5.0$ kPa, and $\delta_{F(B)} = 10.0$ kPa. Both error types introduced into the measurement data had the same resolution (0.1 kPa).

6. RESULTS AND DISCUSSION

We focused exclusively on leak localization while omitting the aspect of the examined procedure's cooperation with a leak detection algorithm. To determine the leak point's coordinate according to dependency (1), we employed the calculations of gradients G_{in} and G_{out}, corresponding to different

configurations of evaporation of pressure transducers. Specifically, we configured pairs of sensors—one located extremely far from the leak point and another located very close to it—following the recommended approach (see Table 1).

Configurations of the pressure transducers used for leak localization in conjunction
with the pressure transducers and the leak point positions

Leak position [m]	Gradients with their corresponding pressures	Position of selected pressure transducers [m]					
		1	61	141	201	281	341
75	$G_{in}(p_{in}, p_n)$	●	●				
	$G_{out}(p_m, p_{out})$			●			●
155	$G_{in}(p_{in}, p_n)$	●		●			
	$G_{out}(p_m, p_{out})$				●		●
235	$G_{in}(p_{in}, p_n)$	●			●		
	$G_{out}(p_m, p_{out})$					●	●

We assessed the accuracy and uncertainty of the calculated leak point using measurement data obtained after reducing the sampling frequency to $f_P = 10$ Hz. The results for individual experiments with simulated single leakages are summarized in Tables 2 and 3. Additionally, Tables 4 and 5 present the averaged absolute location errors for each leak location (denoted as $|error|_{75}$, $|error|_{155}$ and $|error|_{235}$), as well as the overall average error (denoted as $|error|_{all}$). The uncertainty values are also provided (labeled $u(z_u)_{75}$, $u(z_u)_{155}$, $u(z_u)_{235}$ and $u(z_u)_{all}$, respectively).

The results presented in Tables 2–5 refer to the correct state of the measuring system (CSMS) and represent the scenarios where pressure data from this system were affected by specific systematic errors. These errors were deliberately introduced to model real-world conditions. Notably, the impact of these simulated errors may already correspond to the warning state of the measuring system (WSMS).

When performing calculations based on Formulas (1) and (4), we utilized estimated values for individual pressures (p_{in}, p_n, p_m, p_{out}). These values were derived by averaging samples from the sets including $N = 200$ data samples within specific measurement time windows. These windows were positioned at five-second intervals, starting from the moment when the leak was simulated.

Our uncertainty estimation relied on the assumption that the pressure measurement error distribution is centered around the middle of the interval. We assumed this to be a triangular error distribution. Consequently, the uncertainty of type B for measured pressure was expressed as $u_B(p) = \Delta p / \sqrt{6}$. Additionally, for all considered distances, a standard uncertainty of 0.025 m was assumed.

For CSMS, calculated results labeled "CO$_{1/200}$" are supplemented by results labeled "CO$_{3/100}$." The latter values correspond to the same timeframe but were calculated as average values based on the results from three distinct time windows, each covering $N = 100$ data samples and shifted by half the length of a single window [9].

The uncertainty computations, which relate to WSMS, were performed by adopting identical values of the limiting uncertainty Δp corresponding to the input variables p_{in}, p_n, p_m, and p_{out} for the CSMS. This approach corresponded to the assumption that the simulated damage might not be detected in practice by the operator of the measurement system. In general, this was done to determine how the simulated errors resulting in specific changes in the estimated values of these individual pressures would affect the change in the margins of the uncertainty of the calculated coordinate of the leak spot.

The initial step of the investigation was to assess the effectiveness of the examined procedure in terms of the accuracy and uncertainty related to the CSMS. Next, we used these values as the references and compared the results obtained for the specific WSMS with them. These WSMS values are associated

with different types of pressure sensor errors and their various investigated scenarios. This comparison enabled us to evaluate how sensitive these measures are to undesirable events such as sensor errors.

When analyzing the results (labeled "$CO_{1/200}$"), we noticed that the accuracy and uncertainty values for the calculated leak point vary significantly across individual experiments. Generally, the accuracy results range from a fraction (one-tenth) of a meter to several dozen meters. The values of this measure obtained for each of the leaks, which were simulated at the same point in the pipeline, show significant differences. This discrepancy is especially true for the leak point located in the outlet section of the pipeline. Interestingly, not all three considered leak points demonstrate an improvement in localization accuracy with increasing leak intensity, as one might expect. The results in the form of averaged absolute values, which concern individual points, show that the best location results correspond to leaks simulated at the point located in the middle of the pipeline. In contrast, the result for the leak point at the beginning of the pipeline is approximately half as accurate, while the outcome for the point near the end of the analyzed pipeline segment is more than two and a half times worse. Based on this comparison, it should be kept in mind that the location of leaks at each of these three points was carried out based on differently configured pairs of pressure sensors. Hence, the interpretation of these results is less clear than when using identically configured pairs. However, this variant was not considered as not corresponding to the previously mentioned recommendation, and, as it was confirmed by previous studies [9], it may even result in several times worse accuracy of the leak localization. The results related to uncertainty in the case of individual simulated leak locations exhibit significantly less variation. Again, the largest margins of uncertainty were observed for leaks occurring at the end of the pipeline, while the smallest margins were associated with leaks at the beginning of the pipeline. These findings are confirmed by the average values related to specific simulated leak locations. When comparing such results across both investigated measures, along with an overall consideration of all simulated leak locations, it becomes evident that the margins of uncertainty are nearly twice or even three times as large as the averaged absolute values of the location errors. The results labeled "$CO_{1/200}$" and those labeled "$CO_{3/100}$" (which correspond to a different configuration of time windows) are practically identical. The differences between them are a few tenths of a meter. Therefore, observations related to these results, which were previously evaluated alongside other outcomes in research on various implementation variants of the standard gradient-based leak localization procedure, may be useful in this context [9]. Regarding the considered leaks amounting to up to 2% of the nominal flow, the above-mentioned inconsistencies related to the incompletely clear relationships between the accuracy (error) of the location of the leak and its uncertainty in relation to the size of the leak correspond to the observations that can be found in [7]. It is indicated that leaks of such intensity are often completely masked by uncertainties, the source of which may be disturbances in the flow process, measurement noises, or even slight changes in the properties of a pumped fluid.

In the analysis of imitated bias (zero moving) errors, which are detailed for individual experiments (see Table 2), significant changes in leak localization accuracy become evident when compared to the results labeled "$CO_{1/200}$" corresponding to the CSMS. Specifically, for each individually simulated error related to individual sensors, such changes, as they relate to the direction of displacement in the calculated leak point coordinates relative to a base result, were consistent with the patterns depicted in Figs. 6a–d. This alignment is indicated by a specific magnitude Δ. When supplementing observations with average values, which pertain to specific locations of simulated leaks (see Table 4), it becomes much easier to assess the magnitude of these changes. This assessment depends on the error simulation associated with a given pressure transducer and three distinct leak point locations.

In the case of simulated errors at a level of -0.2 kPa, which is twice the resolution of the measurement data, such errors can lead to a change in the calculated leak coordinate of up to several meters. However, when the simulated errors are -0.5 kPa, corresponding to half the uncertainty margin of the pressure transducers used, the accuracy changes compared to results corresponding to lower error levels can be up to twice as large. It is important to clarify that the simulated errors related to the initial pressure sensor p_{in} only cause minor changes in the results.

Table 2

Localization errors and uncertainties depending on the position and intensity of a leak

Leaks		$CO_{3/100}$	$CO_{1/200}$	Bias (i.e., zero moving) type errors $\delta_{F(A)}$ [kPa]							
Position [m]	Intensity [%]			p_{in}		p_n		p_m		p_{out}	
				-0.2	-0.5	-0.2	-0.5	-0.2	-0.5	-0.2	-0.5
75	0.29	−18.5 ±12.9	−18.5 ±12.8	−18.7 ±13.2	−18.9 ±13.8	−20.2 ±12.4	−22.5 ±11.8	−15.9 ±12.8	−12.1 ±12.7	−19.3 ±12.9	−20.5 ±13.0
	0.54	−13.6 ±11.3	−13.7 ±11.3	−13.7 ±11.6	−13.7 ±12.0	−15.3 ±10.9	−17.5 ±10.4	−11.3 ±11.2	−8.2 ±11.2	−14.4 ±11.3	−15.3 ±11.4
	0.83	−5.3 ±10.0	−5.6 ±9.9	−5.4 ±10.1	−5.1 ±10.5	−7.2 ±9.6	−9.4 ±9.3	−3.7 ±9.9	−1.0 ±9.9	−6.1 ±10.0	−6.9 ±10.1
	1.17	−2.1 ±9.2	−1.8 ±9.2	−1.5 ±9.4	−1.1 ±9.8	−3.3 ±9.0	−5.5 ±8.7	−0.3 ±9.2	2.3 ±9.2	−2.4 ±9.3	−2.9 ±9.3
	1.29	0.1 ±9.1	0.3 ±9.0	0.6 ±9.2	1.1 ±9.6	−1.2 ±8.8	−3.4 ±8.5	2.0 ±9.0	4.4 ±9.0	−0.1 ±9.1	−0.7 ±9.1
	1.93	−2.7 ±8.2	−2.6 ±8.2	−2.3 ±8.4	−2.0 ±8.6	−3.9 ±8.0	−5.8 ±7.7	−1.1 ±8.2	1.2 ±8.2	−3.0 ±8.2	−3.6 ±8.3
155	0.24	−3.7 ±21.5	−3.4 ±21.3	−3.2 ±21.8	−2.7 ±22.5	−6.6 ±20.9	−11.3 ±20.2	0.6 ±20.8	6.5 ±20.1	−4.4 ±21.8	−6.3 ±22.6
	0.45	−9.5 ±22.4	−9.5 ±22.0	−9.4 ±22.5	−9.4 ±23.3	−12.8 ±21.5	−17.3 ±20.9	−5.3 ±21.5	1.0 ±20.7	−10.7 ±22.5	−12.9 ±23.4
	0.78	−15.3 ±22.1	−15.7 ±21.8	−15.8 ±22.3	−15.8 ±23.1	−18.7 ±21.4	−23.1 ±20.7	−11.1 ±21.2	−5.0 ±20.5	−17.2 ±22.3	−19.1 ±23.1
	1.20	−0.3 ±13.7	0.2 ±13.4	0.4 ±13.6	0.8 ±13.9	−1.8 ±13.3	−4.9 ±13.0	2.6 ±13.3	6.3 ±13.0	−0.5 ±13.6	−1.4 ±13.9
	1.44	−1.4 ±12.8	−1.1 ±12.6	−1.0 ±12.8	−0.8 ±13.0	−3.2 ±12.5	−6.0 ±12.2	1.3 ±12.5	4.8 ±12.2	−1.7 ±12.8	−2.7 ±13.1
	1.99	−2.5 ±11.8	−2.6 ±11.6	−2.5 ±11.8	−2.4 ±12.0	−4.5 ±11.5	−7.0 ±11.3	−0.4 ±11.5	2.7 ±11.3	−3.3 ±11.8	−4.2 ±12.0
235	0.37	13.8 ±16.9	13.9 ±16.6	14.4 ±16.8	15.2 ±17.0	11.2 ±16.6	7.4 ±16.6	17.1 ±15.8	21.5 ±14.8	12.7 ±17.3	10.7 ±18.5
	0.54	−28.2 ±57.4	−27.4 ±57.2	−27.2 ±58.9	−26.9 ±61.8	−33.6 ±57.0	−42.3 ±56.7	−14.7 ±48.9	0.1 ±40.2	−35.7 ±66.1	−52.8 ±86.3
	0.87	−58.3 ±90.5	−57.4 ±88.1	−58.4 ±92.3	−60.1 ±99.5	−64.5 ±87.2	−74.1 ±85.8	−37.7 ±70.8	−15.4 ±54.2	−74.7 ±110.6	−113.4 ±171.3
	1.28	−5.9 ±29.2	−6.2 ±29.1	−5.7 ±29.6	−5.0 ±30.3	−10.1 ±29.1	−15.7 ±29.1	0.0 ±26.8	8.0 ±23.9	−9.4 ±31.3	−15.0 ±35.3
	1.41	−0.2 ±24.7	0.5 ±24.2	1.1 ±24.5	1.9 ±25.0	−2.9 ±24.2	−7.8 ±24.2	5.5 ±22.6	12.1 ±20.5	−1.9 ±25.8	−6.0 ±28.4
	1.85	−13.0 ±27.4	−12.5 ±27.1	−12.3 ±27.5	−11.6 ±28.1	−15.9 ±27.1	−20.8 ±27.1	−6.6 ±25.1	1.2 ±22.6	−15.6 ±29.0	−21.2 ±32.4

When the errors affect sensors closest to the leak location, denoted as p_n and p_m, the result changes are significantly greater. In general, this applies to all simulated leak sites but is particularly noticeable at the end of the pipeline. When simulated errors concern the final pressure sensor p_{out}, their impact is less marked for leaks simulated at the beginning of the pipeline and slightly more significant for leaks

simulated in the middle section. However, it is most noticeable for leaks located at the end of the pipeline. The results connected to the uncertainty of the calculated leak point generally show a much lower sensitivity of this measure, except regarding the leak location at the end of the investigated pipeline segment and the simulated errors related to sensors p_m and p_{out}.

Table 3

Localization errors and uncertainties depending on the position and intensity of a leak

Leaks		$CO_{3/100}$	$CO_{1/200}$	Proportional ratio type errors $\delta_{F(B)}$ [kPa]					
Position [m]	Intensity [%]			0.2	0.5	1.0	2.0	5.0	10.0
75	0.29	−18.5 ±12.9	−18.5 ±12.8	−18.9 ±12.8	−18.0 ±12.7	−19.1 ±12.8	−18.4 ±12.8	−18.5 ±12.8	−18.7 ±12.6
	0.54	−13.6 ±11.3	−13.7 ±11.3	−14.0 ±11.3	−13.0 ±11.2	−14.2 ±11.2	−13.5 ±11.3	−13.7 ±11.3	−13.9 ±11.1
	0.83	−5.3 ±10.0	−5.6 ±9.9	−6.0 ±9.8	−5.3 ±9.8	−6.1 ±9.8	−5.5 ±9.9	−5.6 ±9.9	−5.6 ±9.8
	1.17	−2.1 ±9.2	−1.8 ±9.2	−2.3 ±9.2	−1.6 ±9.2	−2.4 ±9.2	−1.8 ±9.2	−1.8 ±9.2	−1.9 ±9.1
	1.29	0.1 ±9.1	0.3 ±9.0	0.0 ±9.0	0.6 ±9.0	−0.2 ±8.9	0.5 ±9.1	0.1 ±9.0	0.7 ±9.0
	1.93	−2.7 ±8.2	−2.6 ±8.2	−2.9 ±8.1	−2.3 ±8.1	−3.0 ±8.1	−2.4 ±8.2	−2.4 ±8.1	−2.8 ±8.1
155	0.24	−3.7 ±21.5	−3.4 ±21.3	−4.1 ±21.3	−4.3 ±21.1	−3.8 ±21.3	−3.8 ±21.3	−2.2 ±21.1	−4.0 ±21.1
	0.45	−9.5 ±22.4	−9.5 ±22.0	−10.1 ±22.1	−10.3 ±21.7	−9.9 ±22.0	−9.9 ±22.0	−8.6 ±21.8	−9.1 ±21.7
	0.78	−15.3 ±22.1	−15.7 ±21.8	−16.5 ±22.0	−16.4 ±21.6	−16.2 ±22.0	−16.0 ±21.8	−15.4 ±21.5	−15.3 ±21.5
	1.20	−0.3 ±13.7	0.2 ±13.4	−0.1 ±13.4	−0.4 ±13.3	−0.2 ±13.4	−0.2 ±13.4	0.7 ±13.3	0.0 ±13.3
	1.44	−1.4 ±12.8	−1.1 ±12.6	−1.5 ±12.6	−1.6 ±12.5	−1.3 ±12.6	−1.3 ±12.6	−1.4 ±12.5	−1.0 ±12.5
	1.99	−2.5 ±11.8	−2.6 ±11.6	−3.0 ±11.7	−3.3 ±11.6	−2.9 ±11.7	−2.8 ±11.6	−2.9 ±11.6	−3.1 ±11.6
235	0.37	13.8 ±16.9	13.9 ±16.6	14.7 ±16.5	14.4 ±16.4	14.5 ±16.5	14.2 ±16.5	14.2 ±16.4	14.2 ±16.3
	0.54	−28.2 ±57.4	−27.4 ±57.2	−24.8 ±55.6	−24.6 ±54.8	−24.9 ±56.0	−26.3 ±56.5	−26.7 ±55.4	−28.8 ±57.4
	0.87	−58.3 ±90.5	−57.4 ±88.1	−53.1 ±85.7	−52.5 ±82.7	−54.8 ±87.1	−56.3 ±87.3	−56.9 ±86.1	−60.5 ±88.9
	1.28	−5.9 ±29.2	−6.2 ±29.1	−4.5 ±28.9	−5.0 ±28.5	−4.9 ±29.0	−5.7 ±29.0	−6.2 ±28.9	−7.6 ±29.2
	1.41	−0.2 ±24.7	0.5 ±24.2	2.0 ±24.0	1.5 ±23.8	1.6 ±24.2	0.8 ±24.1	0.3 ±24.2	−0.3 ±24.2
	1.85	−13.0 ±27.4	−12.5 ±27.1	−10.9 ±26.9	−11.2 ±26.5	−11.6 ±27.1	−11.9 ±27.0	−13.9 ±27.7	−12.5 ±26.9

Table 4

Averaged absolute values of localization errors and averaged values of localization uncertainties depending on the leak location

Leaks in relation to leak location	$CO_{3/100}$	$CO_{1/200}$	Bias (i.e., zero moving) type errors $\delta_{F(A)}$[kPa]							
			p_{in}		p_n		p_m		p_{out}	
			-0.2	-0.5	-0.2	-0.5	-0.2	-0.5	-0.2	-0.5
$|error|_{75}$	7.1	7.1	7.0	7.0	8.5	10.7	5.7	4.9	7.6	8.3
$u(z_u)_{75}$	±10.1	±10.1	±10.3	±10.7	±9.8	±9.4	±10.0	±10.0	±10.1	±10.2
$|error|_{155}$	5.6	5.4	5.4	5.3	7.9	11.6	3.6	4.4	6.3	7.8
$u(z_u)_{155}$	±17.4	±17.1	±17.5	±18.0	±16.8	±16.4	±16.8	±16.3	±17.5	±18.0
$|error|_{235}$	20.1	19.6	19.8	20.1	23.0	28.0	13.6	9.7	25.0	36.5
$u(z_u)_{235}$	±41.0	±40.4	±41.6	±43.6	±40.2	±39.9	±35.0	±29.4	±46.7	±62.0
$|error|_{all}$	10.9	10.7	10.8	10.8	13.2	16.8	7.6	6.3	13.0	17.5
$u(z_u)_{all}$	±22.8	±22.5	±23.1	±24.1	±22.3	±21.9	±20.6	±18.6	±24.8	±30.1

Table 5

Averaged absolute values of localization errors and averaged values of localization uncertainties depending on the leak location

Leaks in relation to leak location	$CO_{3/100}$	$CO_{1/200}$	Proportional ratio type errors $\delta_{F(B)}$[kPa]					
			p_{in}, p_n, p_m, p_{out}					
			0.2	0.5	1.0	2.0	5.0	10.0
$|error|_{75}$	7.1	7.1	7.3	6.8	7.5	7.0	7.0	7.3
$u(z_u)_{75}$	±10.1	±10.1	±10.0	±10.0	±10.0	±10.1	±10.1	±10.0
$|error|_{155}$	5.6	5.4	5.9	6.0	5.7	5.7	5.2	5.4
$u(z_u)_{155}$	±17.4	±17.1	±17.2	±17.0	±17.2	±17.1	±17.0	±16.9
$|error|_{235}$	20.1	19.6	18.3	18.2	18.7	19.2	19.7	20.6
$u(z_u)_{235}$	±41.0	±40.4	±39.6	±38.8	±40.0	±40.1	±39.8	±40.5
$|error|_{all}$	10.9	10.7	10.5	10.4	10.6	10.6	10.6	11.1
$u(z_u)_{all}$	±22.8	±22.5	±22.3	±21.9	±22.4	±22.4	±22.3	±22.5

When evaluating the results related to the imitated gain-type errors, it is worth bearing in mind that the occurrence of such errors, when using pressure transducers characterized by identical input ranges, theoretically should not cause a change in the calculated leak location. This is demonstrated in Fig. 6b.

However, for the researched error levels, the results related to individual experiments (see Table 3) and the average values for specific leak locations (see Table 5) did not fully confirm this finding. Although the results for the considered error levels characterized by the magnitude $\delta_{F(B)}$ slightly differ from each other, they do not demonstrate evident changes compared to the results labeled "$CO_{1/200}$" corresponding to the CSMS. This could be because, for different investigated error levels, numerically simulated with a resolution corresponding to the measurement data, their uniform impact across the entire measurement range may not be reached. As a result, the anticipated occurrence of such errors for all pressure transducers may not be achieved.

It is essential to acknowledge that simulating systematic errors, which can be challenging to execute practically, has been replaced with numerically induced alterations in the measurement data gathered during tests with simulated leakages. Thus, a similar study employing a computational pipeline model should be considered. Such an approach would give clarity when simulating errors corresponding to both the CSMS and WSMS. It is also possible to obtain results that would serve as a reference to those

presented in this paper. This would allow for the development of comprehensive maps (distributions) determining the impact of errors on both considered measures related to the examined leak localization procedure, taking into account the different locations of leaks and their intensity, even up to the level of 10% of the nominal flow.
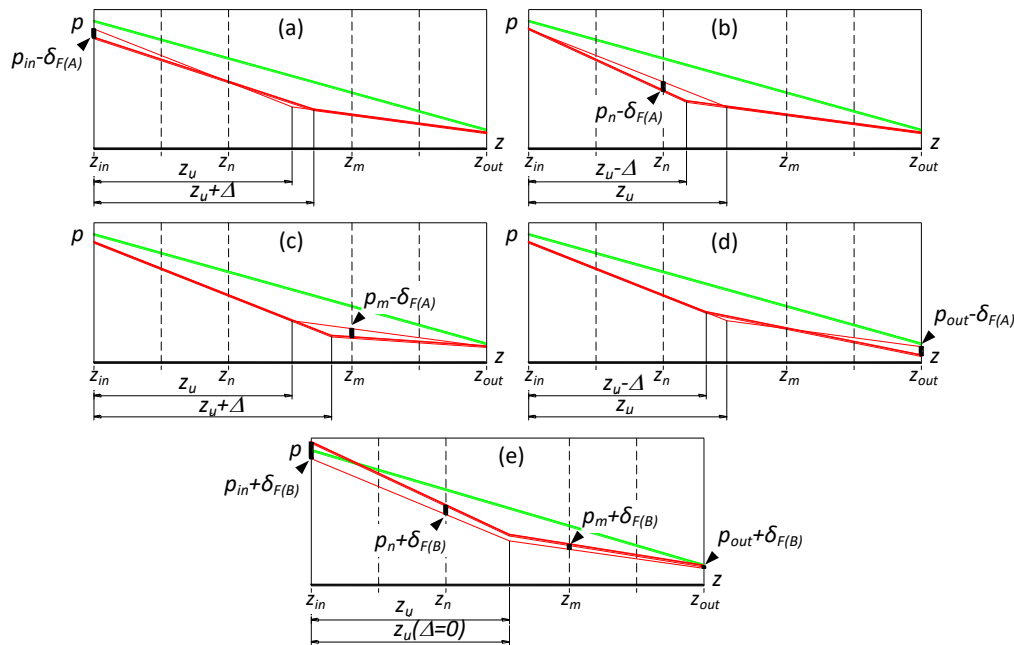
Fig. 6. Relation between the leak point coordinates obtained for the CSMS and its changes caused by (a)-(d) bias (zero moving) type errors corresponding to individual transducers and (e) gain type errors related to all transducers

7. CONCLUSIONS

This experimental point assessment of the sensitivity of the standard gradient-based leak localization procedure investigated how the procedure responds to common static systematic errors associated with analogue pressure transducers. Specifically, it focused on the accuracy and uncertainty of the resultant coordinate of the leak point. A laboratory water pipeline was used to examine the procedure's ability to locate small leaks (with intensities ranging from 0.25% to 2.00% of the nominal flow rate) at different sections of the pipe (inlet, middle, and outlet). The study provides information on the sensitivity of accuracy and uncertainty measures to specific levels of considered errors and combinations of their occurrence for selected pressure sensors. The results indicate the specific consequences of both types of errors under consideration. Additionally, they pinpointed certain problems that will be studied in future work.

Acknowledgement

References

1. Amori, K.E. & Al-Salmany, Z. Solid particle erosion in the sudden contraction of raw water pipeline. *Diagnostyka*. 2022. Vol. 23. No. 1. P. 1-13.

2. Benallou, I. & Azmani, A. & Azmani, M. & Atik El Ftouh, M. Optimizing transportation systems and mitigating risks: a comprehensive analysis of distribution supply chain challenges. *Scientific Journal of Silesian University of Technology. Series Transport*. 2023. 121. P. 19-30.

3. Chen, R. & Cui, S. & Khoo, D.W.Y. & Khoo, B.C. Modelling and quantification of measurement uncertainty for leak localisation in a gas pipeline. *Measurement: Sensors*. 2022. Vol. 24. No. 100443.

4. Droździel, P. & Vitenko, T. & Zhovtulia, L. & Yavorskyi, A. & Oliinyk, A. & Rybitskyi, I. & Poberezhny, L. & Popovych, P. & Shevchuk, O. & Popovych, V. Non-contact method of estimation of stress-strain state of underground pipelines during transportation of oil and gas. *Scientific Journal of Silesian University of Technology. Series Transport*. 2020. Vol. 109. P. 17-32.

5. Duan, H.F. Uncertainty analysis of transient flow modeling and transient-based leak detection in elastic water pipeline systems. *Water Resour Manage*. 2015. Vol. 29. P. 5413-5427.

6. Korlapati, N.V.S. & Khan, F. & Noor, Q. & Mirza, S. & Vaddiraju, S. Review and analysis of pipeline leak detection methods. *Journal of Pipeline Science and Engineering*. 2022. Vol. 2. No. 100074.

7. Lu, Z. & She, Y., Loewen, M. A sensitivity analysis of a computer model-based leak detection system for oil pipelines. *Energies*. 2017. Vol. 10. No. 1226.

8. Michnej, M. & Młynarski, S. & Pilch, R. & Sikora, W. & Smolnik, M. & Drożyner, P. Physical and reliability aspects of high-pressure ammonia water pipeline failures. *Eksploatacja i Niezawodnosc – Maintenance and Reliability*. 2022. Vol. 24(4). P. 728-737.

9. Ostapkowicz, P. & Bratek, A. Accuracy and uncertainty of gradient based leak localization procedure for liquid transmission pipelines. *Sensors*. 2021. Vol. 21. No. 5080.

10. Sekhavati, J. & Hashemabadi, S.H. & Soroush, M. Computational methods for pipeline leakage detection and localization: A review and comparative study. *Journal of Loss Prevention in the Process Industries*. 2022. Vol. 77. No. 104771.

11. Troitskiy, V. News in maintenance of technical state of the main pipelines. *Nondestructive testing and diagnostics*. 2018. Vol. 2. P. 37-44.

12. Turkowski, M. & Bratek, A. & Ostapkowicz, P. Uncertainty analysis as the tool to assess the quality of leak detection and localization systems. In: *Recent Global Research and Education: Technological Challenges*. Advances in Intelligent Systems and Computing 519. Springer International Publishing AG 2017. P. 469-475.

13. Wang, Y. & Xie, MJ. & Su, C. Dynamic reliability evaluation of buried corroded pipeline under rockfall impact. *Eksploatacja i Niezawodnosc – Maintenance and Reliability*. 2022. Vol. 24(2). P. 275-288.

14. Zachwieja, J. & Gawda, M. Properties diagnosing of dynamic pipeline-pomp system in terms of vibration damping possibility. *Diagnostyka*. 2006. Vol. 40. No. 4. P. 27-31.

15. *Evaluation of the Measurement Data: Guide to the Expression of Uncertainty in Measurement (GUM 1995 with minor corections)*. Joint Committee for Guides in Metrology 100: 2008, BIPM, Sĕvres, Frnace.

16. ISO 5168:2005. *Measurement of Fluid Flow–Evaluation of Uncertainties*. ISO: London, UK, 2005.